Pre-print of: Recillas, S. et al. "Use of CeO_2, TiO_2 and Fe_3O_4 nanoparticles for the removal of lead from water. Toxicity of nanoparticles and derived compounds" in Desalination (Ed. Elsevier), vol. 277, issues 1-3 (Aug. 2011), p. 213-220. The final version is available at DOI 10.1016/j.desal.2011.04.036

Use of CeO_2, TiO_2 and Fe_3O_4 nanoparticles for the removal of lead from water. Toxicity of nanoparticles and derived compounds.

Sonia Recillas[1], Ana García[1], Edgar González[2], Eudald Casals[2], Victor Puntes[2,3], Antoni Sánchez[1,*], Xavier Font[1]

1. Department of Chemical Engineering, Escola d'Enginyeria, Universitat Autònoma de Barcelona, 08193 Bellaterra, Spain

2. Institut Català de Nanotecnologia, Campus de la Universitat Autònoma de Barcelona, 08193 Bellaterra, Spain

3. Insitut Català de Recerca i Estudis Avançats, Passeig Lluís Companys, 23, 08010 Barcelona, Spain

*Corresponding author: Antoni Sánchez

Phone: 34-935811019

Fax: 34-935812013

E-mail address: antoni.sanchez@uab.cat

Abstract

Nanoparticles (NPs) suspensions of CeO_2, Fe_3O_4 and TiO_2 were synthesized and tested for lead removal in water cleaning processes. The results obtained are promising for the use of these NPs in lead elimination via adsorption process. The adsorption capacity obtained for the NPs was: 189 mg Pb/g NPs CeO_2, 83 mg Pb/g NPs Fe_3O_4 and 159 mg Pb/g NPs TiO_2. Another important issue assessed in this study was to determine the toxicity of the NPs in each step of the process: synthesized NPs, NPs after lead adsorption and the supernatant after NPs separation. In order to study the interaction with living organisms and prevent future environmental damages, the Germination test in Tomato (*Lycopersicom esculentum)*, Lettuce (*Lactuca sativa)*, Cucumber *(Cucumis sativus)* seeds and the Microtox® assay, based on the use of bioluminescent marine bacterium, *Photobacterium phosphoreum/Vibrio fischeri*, were used to evaluate the toxicity of these materials. The CeO_2 NPs showed a high level of lead removal although presented a high phytotoxicity. The TiO_2 NPs inhibited the lead toxicity against the marine bacterium. Interestingly, the media used to stabilize the NPs (tetramethylammonium hydroxide and hexamethylenetetramine) presented a significant reduction in the germination index. TiO_2 and Fe_3O_4 NPs did not exhibit any toxicity and could be used as absorbents for Pb (II) removal.

Keywords: Lead adsorption; Nanoparticles; Toxicity; Phytotoxicity; Water Treatment.

1. Introduction

The use of nanoparticles (NPs) for water treatment processes is now a reality: a long list of materials based on nanostructures are today in the market or under final research steps [1], even though the worldwide tendency to decrease the permitted level of contamination in drinking water is a big challenge for the environmental researchers [2]. In the case of lead contamination, the toxicity and poisoning by lead in numerous areas are well documented [3,4]. Many methods have been used to remove Pb (II) from water and waste-water, mainly by chemical precipitation, ionic exchange, membrane separation, biosorption, adsorption process, etc. However, most of them require an extensive processing and present a high cost. It is therefore necessary to develop more efficient remediation strategies that are able to remove Pb (II) from contaminated water at high concentrations [5].

The main advantage of using NPs materials compared to conventional materials is the high surface area, which means a large space for the development of chemical reactions, physic interchanges, etc. [6]. Nevertheless, the use of these materials in any application has to consider this high surface reactivity in order to prevent possible ecological damage. In recent years, substantial attention has been paid to the environmental damage evaluation [7,8], although a lot of answers about the NPs toxic effects are still unknown [9]. The toxicity of a considerable number of NPs used for water treatment has been reported in the literature using different methodologies [10,11], although the complete removal process in which the NPs are involved (i.e. adsorption, ionic exchange, etc.) and the physicochemical and structural changes during the process have not been exhaustively studied. The effects and toxicity mechanisms of NPs on plants have been in fact poorly studied [12,13]. Other important issue is the

difficulty to compare the adsorption capacity of nanomaterials reported in the literature because the experimental reaction conditions and the surface chemistry of NPs are not always the same [14].

In the present work, the adsorption capacity at different lead concentrations, the kinetic adsorption behavior at 100 mg/ml of lead concentration in front of CeO_2, TiO_2 and Fe_3O_4 NPs suspensions at the same concentration (320 mg/l) and similar order of particle size have been studied. The toxicity of the initial CeO_2, Fe_3O_4 and TiO_2 NPs suspensions, the NPs after lead adsorption process separated by centrifugation and the water remaining after NPs separation were evaluated by the bioluminescent bacteria test (Microtox) and the germination test as standard toxicity tests.

2. Materials and Methods

2.1. Synthesis of Nanoparticles (NPs)

Different kinds of metallic and metal oxide NPs were synthesized in aqueous phase, using milli-Q grade water. All reagents were purchased from Sigma-Aldrich and used as received. All the synthesis procedures are based on preexisted ones available in the scientific literature with modifications to be adapted to large-scale yields. For CeO_2 NPs, a method based on Zhang et al. [15] was used. The Ce^{3+} ions from $Ce(NO_3)_3$ salt were oxidized at basic pH conditions to Ce^{4+} using Hexamethylenetetramine (HMT). Then, the CeO_2 nanocrystals precipitate and are further stabilized in aqueous solution with the same reagent (HMT), which forms the double electrical layer to prevent NPs agglomeration.

For the synthesis of TiO_2, the process of Pottier et al. [16] was used. The synthesis procedure consists on the decomposition of Titanium Tetrachloride ($TiCl_4$) at acidic pH (from 2 to 6). After this, it follows a growing step of the nanocrystals, carried

out in an oven at 70ºC, a purification step by centrifugation and a resuspension with tetramethylammonium hydroxide (TMAOH) to stabilize the NPs. Depending on the pH used during the growing step, the obtained size and shape of the TiO_2 varies from small size and spherical-like NPs (from 5 nm, not used in this work) to bigger particles (around 10 nm, pH = 5, used in this work).

For Fe_3O_4 NPs, they were synthesized by a modified method based on Massart's method [17,18]: amounts of 1 mmol iron (II) chloride ($FeCl_2$) and 2 mmol iron (III) chloride ($FeCl_3$) were dissolved in 50 mL deoxygenated water and then added dropwise to 50 mL of a solution of 1 M deoxygenated TMAOH. After 30 min of vigorous stirring under a N_2 stream, the Fe_3O_4 precipitate was washed by soft magnetic decantation and redissolved in 1 mM TMAOH to obtain the final stable colloidal solution of Fe_3O_4 NPs. Table 1 shows the main characteristics of the NPs used in this work.

2.2. Characterization and stability of NPs

All NPs were characterized using different techniques: Transmission Electron Microscopy (TEM), Zeta Potential (Z-Potential), Dynamic Light Scattering (DLS) and X-Ray Diffraction (XRD). TEM images were acquired with a JEOL 1010 Electron Microscope operating at an accelerating voltage of 80 kV. Samples for TEM were prepared by drop casting on carbon coated cooper TEM grids and left solvent evaporate at room temperature. Afterwards, more than 500 particles from different images were computer-analyzed and measured for size distribution analysis.

Z-Potential and DLS measurements were made with a Malvern ZetaSizer Nano ZS Instrument operating at a light source wavelength of 532 nm and a fixed scattering angle of 173° for detection. Aliquots of 0.8 ml of the colloidal NPs solutions were placed into the specific cuvette and the software was arranged with the specific

parameters of refractive index and absorption coefficient of NP material and solvent viscosity (data required to obtain the correct value for each NP type). Z-Potential is a commonly used tool to determine the stability of a colloidal suspension of electrostatically stabilized NPs as the ones used in this work. DLS allows the determination of the hydrodynamic diameter of colloidal particles, which is the diameter of the sphere with the same Brownian motion as the analyzed particle, and is also used to check for the presence of agglomerates.

X-Ray Diffraction (XRD) spectra were acquired with a PANalytical X'Pert diffractometer that uses a Cu Kα radiation source. Samples for XRD consist of the dry NPs in powder form. For this purpose, NPs were extracted out of the colloid through centrifugation and recovering and drying the pelleted powder NPs (Table 1 and Fig. 1).

2.3. Pb^{2+} Adsorption studies

The adsorption kinetics and the adsorption capacity (qe) at equilibrium of Fe_3O_4, TiO_2 and CeO_2 NPs synthesized at room temperature and pH = 7 were performed by the following procedure. A solution of 200 mg/l of Pb^{2+} was prepared by dissolving the required amount of $Pb(NO_3)_2$ in deionized water.

The NPs of Fe_3O_4 and TiO_2 were diluted in deionized water to obtain the same concentration of CeO_2 NPs (640 mg/l). The pH of each NPs suspension was adjusted at 7 using sodium hydroxide 0.1 M (CeO_2 NPs) and citric acid 0.1 M (Fe_3O_4 NPs and TiO_2 NPs). Then 25 ml of lead solution (200 mg/l) was poured in a bottle and afterwards, 25 ml of each NPs suspension was added drop by drop to the bottle. Finally, the suspension was continuously stirred at 150 rpm at room temperature. The samples obtained at different times were centrifuged. The lead concentration from the liquid phase was determined by a standard colorimetric method [19]. Experiments were carried out in

triplicate and the average values are presented. Standard deviation values were always lower than 4%. From this solution the other ones were prepared by doing the appropriated dilutions.

2.4. Pb^{2+} Adsorption isotherm experiments

The adsorption isotherm experiments were carried out with lead solutions at different initial Pb^{2+} concentrations (3.4 mg/l Pb^{2+}, 8.5 mg/l Pb^{2+}, 17 mg/l Pb^{2+}) at pH 7 and at room temperature (Table 2). The experimental procedure was the same used to obtain the adsorption kinetics. The initial and final lead concentration from the liquid phase was determined by a standard colorimetric method. To assure the equilibrium and guarantee the full adsorption, the NPs suspensions were centrifuged after 24 h of adsorption time. The equilibrium time is in agreement with other reports [20] for the adsorption of lead by magnetic nanoadsorbents and for the adsorption of others metal ions onto iron oxide nanoparticles [21-23].

2.5. Bioluminescent test

A commercial Microtox Analyzer model 500 from Azur Environmental was used. Whole Effluent Toxicity (WET) test protocol was used to determine the toxicity of the initial lead solution (2.5 mg/l), the initial NPs suspensions of CeO_2, Fe_3O_4, TiO_2 of 320 mg/l and the final suspension obtained after 3 h of adsorption process at pH 7 and at room temperature.

The Microtox test is based on the percentage of decrease in the amount of light emitted by the bioluminescent marine bacterium *Vibrio fischeri* (*Photobacterium phosphoreum*) [24,25]. The light emitted reduction is directly related to the relative toxicity of the sample. For the three suspensions the half maximal inhibitory

concentration (IC50) was calculated. IC50 is a measure of the effectiveness of a compound in inhibiting biological or biochemical functions and it was obtained from plotting the percentage of luminescence reduction against concentration after 15 min incubation time. It is considered that if IC50 (%) ≤ 25 the suspension is highly toxic; within 25-50 the suspension is moderately toxic; within 51-75 the suspension is toxic; for values higher than 75 the suspension is slightly toxic and for values higher than 100 the suspension is non-toxic [26]. The experimental procedure has been adopted from the official standards of several countries [27,28].

The NPs synthesized (NPs Fe, NPs Ce, NPs Ti), the NPs after 24 h adsorption process (NPs Fe+Pb, NPs Ce+Pb, NPs Ti+Pb), the liquid obtained after the NPs centrifugation (liquor NPs Fe, liquor NPs Ce, liquor NPs Ti) and the initial lead solution (2.5 mg/l) were evaluated following the Microtox test.

Toxicity tests for stabilizer samples and NPs suspensions samples were performed in triplicate. pH of stabilizers and NPs suspension samples was previously adjusted to 7. No visible precipitate was observed during the adjustment.

2.6. Seed germination test

The phytotoxicity of the NPs used for the adsorption studies (CeO_2, TiO_2, Fe_3O_4), the NPs after adsorption process (NPs plus Pb), the liquid obtained after the NPs centrifugation (NPs plus Pb adsorption resulting liquor), the medium containing the stabilizer, a pure medium used with 2.5 mg/l lead solution (medium plus Pb) and deionized water as a control was evaluated by the germination test on Tomato (*Lycopersicom esculentum*), Lettuce (*Lactuca sativa*) and Cucumber (*Cucumis sativus*) seeds. The experiments were performed at 25ºC (pH = 7) in triplicate.

Twenty seeds of tomato, twenty seeds of lettuce and ten seeds of cucumber were

evaluated using the germination test described by Tiquia et al. [29]. 4 ml of the NPs suspension or solutions tested were poured in Petri dishes with a Whatman Nº1 filter paper. The experiments were performed in the dark. After 5 incubation days, the seed germination, the root elongation and the germination index were determined. Each of experimental values was compared with its corresponding control. All the statistical analysis was performed using the software SPSS 17.0 (SPSS Inc., Chicago, USA). Statistical significance was considered for a confidence level of 95% in all the statistical analyses. Relative root elongation (E) and germination index (GI) were calculated according to standard methods [30], as reported below:

GI= (% seed germination)(% root elongation)/100

where:

% seed germination = (Seeds germinated with NPs)/(Seeds germinated with control)x100

% root elongation (E) = (Mean root length with NPs)/(Mean root length with control)x100

3. Results and discussion

3.1. Nanoparticles characterization

The morphology and size distribution of nanoparticles were characterized by TEM (Fig. 1). TEM image of CeO_2 nanoparticles with octahedral morphology and XRD pattern are shown. The diffraction peaks are corresponding to the (111), (200), (220), (311), (222), (400), (331) and (420) planes for the cubic fluorite structure of CeO_2. The average diameter of nanoparticles is 12.4 nm. In the case of TiO_2 nanoparticles, TEM

image (Fig. 1) indicates that the average size of NPs is about 7.6 nm and the shape of product is amorphous. XRD pattern shows the diffraction peaks corresponding to the (111), (101), (111), (210), (211), (220), (002), (301) and (112) planes, respectively. Finally, TEM image of Fe_3O_4 nanoparticles shows an average diameter of 7.8 nm whereas XRD pattern presents the diffraction peaks in (220), (311), (400), (422), (511) and (400) planes, which correspond to the standard pattern of Fe_3O_4. In general, all the nanoparticles show an irregular morphology.

Other general characteristics of the nanoparticles used in this study are presented in Table 1. In this Table, it is important to emphasize to value of the Z-potential to compare it with other published works, since these parameter is strongly affected by the media used to stabilize the nanoparticles and to prevent their agglomeration, a point that is not often considered when working with commercial nanoparticles powders [2,24].

3.2. Adsorption Kinetics

The adsorption evolution obtained for TiO_2, Fe_3O_4 and CeO_2 NPs is shown in Fig. 2. In the case of Fe_3O_4 and CeO_2 NPs, the maximum adsorption was reached almost immediately at the first measure (15 minutes), while the maximum adsorption in the case of TiO_2 NPs was reached after an oscillation period of adsorption-desorption (being this oscillation behavior close to the analytical method precision). After around 10 h the three systems reached equilibrium and were stable with time. The percentages of removal after 24 h of adsorption and 100 mg/l Pb^{2+} of initial concentration were: 58% for CeO_2, 49% for TiO_2 and 26% for Fe_3O_4. Experiments at different initial Pb^{2+} concentration were performed to evaluate the adsorption capacities of the NPs studied. The sorption equilibrium capacity (q_e) of the adsorbed Pb^{2+} was calculated according to the following equation:

$$q_e = (C_0\text{-}C_e)V/m \qquad \text{Eq. (1)}$$

where: C_0 and C_e represent the initial and equilibrium metal ion concentration (mg/l), respectively; V is the volume of the metal ion solution (mL), and *m* is the amount of adsorbent (mg) (Table 2).

The sorption equilibrium capacity (q_e) obtained for 95 mg/l initial concentration of Pb^{2+} were: 181.2 mg Pb^{2+}/g NPs CeO_2, 153.24 mg Pb^{2+}/g NPs TiO_2 and 81.6 mg Pb^{2+}/g NPs Fe_3O_4 (Table 2). The Fe_3O_4 NPs completely removed the Pb^{2+} up to 17 mg/l Pb^{2+}, the CeO_2 NPs removed completely the Pb^{2+} up to 8.5 mg/l and the TiO_2 NPs up to 3.4 mg/l.

In order to investigate the adsorption kinetic of Pb^{2+} with the nanoadsorbents, two kinetics models were applied to simulate the experimental results (pseudo-first-order and pseudo-second-order models). The linear form of pseudo-first-order model can be expressed as:

$$\log (q_e\text{-}q_t) = \log q_e - (k_1/2.303)t \qquad \text{Eq. (2)}$$

where: q_e and q_t (mg/g) are the amounts of the metal ions adsorbed at equilibrium (mg/g) and at time t (h), respectively, and k_1 is the pseudo-first-order rate constant (h^{-1}). The adsorption rate constant (k_1) can be determined experimentally by plotting log ($q_e - q_t$) versus t. The correlation coefficient values R^2 obtained plotting the log ($q_e - q_t$) versus t for each NPs experiment data was very low (NPs TiO_2 0.6914, NPs CeO_2 0.5166, NPs Fe_3O_4 0.2911). These results suggest that the adsorption of Pb^{2+} onto the NPs studied did not follow pseudo-first order-kinetics.

3.3. Pseudo-second-order kinetic model

In recent years, the pseudo-second-order rate expression has been widely applied to the adsorption of pollutants from aqueous solutions [31]. In consequence, a pseudo-second-order model based on the assumption that the rate limiting step are the chemical sorption involving valence forces through sharing or the exchange of electrons between sorbent and sorbate [32] was used as kinetic model. The kinetics of the sorption reaction has been described as a function of the sorption equilibrium capacity (q_e), the initial metal ion concentration, the adsorbent dose and the nature of the solute ion.

The pseudo-second-order rate constants (k_2) and the amount of Pb^{2+} adsorbed at equilibrium (q_e) were calculated experimentally by plotting (t/q_t) versus t according to Equation 3, where q_e is the amount of Pb^{2+} adsorbed (mg/g NPs) at equilibrium, while q_t is the amount of the adsorption (mg/g) at any time t.

$$t/q_t = 1/k_2 q^2_e + (1/q_e)t \qquad \text{Eq. (3)}$$

Fitted equilibrium adsorption capacities (q_e) derived from Equation 3 are similar and in close agreement with those observed experimentally in the case of the three NPs studied (Table 3, Fig. 3). The correlation coefficient (R^2) for the pseudo-second-order kinetic model fits are: 0.991 for CeO_2, 0.986 for Fe_3O_4 and 0.982 for TiO_2. The differences between the experimental sorption equilibrium capacity and the value obtained by the pseudo-second-order kinetic model was less than 4% in the three cases; this suggest that lead adsorption followed pseudo-second-order kinetics and Pb ions were adsorbed onto the CeO_2, TiO_2 and Fe_3O_4 surface via chemical interactions. To make a comparison between adsorption capacities of NPs many variables are to be taken into account: synthesis methodology, reaction conditions, precursors used,

stabilizers molecules, etc., which contribute to have different chemical surface groups, surface imperfections, impurities, changes in morphology nanoparticles size between others. Also the methodology used to obtain the adsorption capacities is variable. Even though, a rough comparison between the adsorption capacities of similar NPs could be done. Nashaat and Nassar [20] reported a maximum adsorption capacity of Pb^{2+} onto Iron Oxide Nanoparticles equal to 36 mg/g for particles size between 20-30 nm. The high adsorption capacity obtained by the Fe_3O_4 nanoparticles synthesized (81.6 mg/g) could be explained by the smaller nanoparticles size and size distribution, which allows more reactive surface sites and disorders surface regions favorable to adsorb Pb^{2+} (Fig. 1). Differences in adsorption capacities of TiO_2 NPs were observed in the literature: TiO_2 rutile phase q_{Pb}=2260 µg/g, NPs diameter 5-40 nm [33] and TiO_2 nanocomposites of TiO_2/multiwalled carbon nanotubes q_{max} = 137 mg/g [34]. In the case of the TiO_2 NPs synthesized, the large capacity obtained could be attributed to the smaller particle size and the homogeneous size distribution (Fig. 1).

The stabilization agents are essential for the stability of the colloids and their presence in the NPs formulation could not be avoided. These ions are loosely attached to the NPs, i.e. there is no a covalent bond between the surface of NPs and the ions and thus, NPs electrostatically stabilized are recognized to have a “naked” surface and do not have a role in the adsorption process.

3.4. Bioluminescent test results

The bioluminescent test is broadly used to evaluate the potential harmful effects of effluents discharged into surface waters [35]. The IC50 (Table 4) obtained for the Fe_3O_4 NPs suspension was 44.8 mg/l, Fe_3O_4 NPs with lead adsorbed (2.5 mg/l Pb^{2+} initial concentration) presented a value of 55 mg/l and for the liquor obtained after the

centrifugation of the Fe_3O_4 NPs with lead adsorbed, IC50 was 144 mg/l. In the case of CeO_2 NPs the IC50 value obtained was 35.2 mg/l. IC50 for NPs CeO_2 with lead adsorbed was 38.7 mg/l and for the liquor obtained after the centrifugation of the CeO_2 NPs with lead adsorbed was 35.2 mg/l. All the measurements were obtained at 15 min of exposure time.

No significant changes in toxicity were observed between the NPs of Fe_3O_4 and NPs of Fe_3O_4 with lead adsorbed. The toxicity of the liquor of Fe_3O_4 with lead adsorbed evaluated after centrifugation process decreased considerably. In the case of CeO_2 NPs and the NPs with lead adsorbed in the structure, no significant differences were observed. These results, obtained for Fe and Ce NPs, indicate that the adsorbed Pb on the NPs does not have any toxicity effect. However, when the NPs of CeO_2 with lead adsorbed were centrifuged and the liquor tested, similar toxicity was obtained. This result could be explained by the nanoparticles dissolution process that could liberate toxic compounds.

The TiO_2 NPs with adsorbed lead and the liquor obtained after the centrifugation of the TiO_2 NPs presented in all cases a slight diminution that were less than 40% at an interval of concentration within 19.4 to 322.5 mg/l of TiO_2 NPs. These results are indicative of the non-toxic effect of TiO_2 NPs against the *Photobacterium phosphoreum* marine bacteria in accordance with several reports available in the literature related to the relatively low toxicity [36,37] of TiO_2 NPs. Even though the high toxicity of the lead solution (Table 4), the NPs with lead adsorbed presented no toxic effect. The TiO_2 NPs has been previously used to pre-concentrate lead in river water and seawater to measure the concentration in water, although the interaction of the nanoparticle and lead was not studied [9]. The Microtox results obtained pointed out a synergic interrelation between the TiO_2 NPs and the lead adsorbed, reducing the toxic effect of lead against

Photobacterium phosphoreum bacteria (Table 4), similarly to that described for Fe_3O_4 and CeO_2 NPs. Pärt and Wilmark [37] have suggested that some organisms have a low uptake of chelated metals and biological membranes that are impermeable to metal-ethylenediaminetetraacetic acid (EDTA) and nitrilotriacetic acid (NTA) chelates reducing the metal toxicity [37]. In this case, the complex formation on the NPs surface with the lead cation could explain the decrease in the toxicity of lead [38,39].

3.5. Seed germination tests results

The phytotoxicity results obtained for the Fe_3O_4, TiO_2 and CeO_2 NPs tested on lettuce, cucumber and tomato are shown in Table 5. In all cases, Pb^{2+} concentration was 2.5 mg/l.

3.5.1. Fe_3O_4 NPs

Significant reduction on lettuce germination index (GI) were detected in the samples containing TMAOH medium (61±1 %) and TMAOH medium with 2.5 mg/l Pb^{2+} in solution (64±2 %); in the case of tomato the effect was more accentuated with 42±12 % and 41±5 % values of GI, respectively. In the samples containing the NPs suspension a negative effect was observed in tomato seeds for both, the NPs suspension used (61±3 %) and the NPs with lead adsorbed (67±15 %). In the case of cucumber seeds, the reduction in the germination index and root elongation was not significant in all the samples tested. The germination index of lettuce, tomato and cucumber seeds were not affected by the liquor obtained after the centrifugation process.

The negative effect obtained in the GI was associated to the root elongation decrease (Table 5). The TMAOH medium affected negatively the root elongation in tomato and lettuce seeds. In fact, the diminution in the germination index and root

elongation can be attributed to the TMAOH medium. The 2.5 mg/l lead solution did not affect the germination index. The differences in the GI between the medium sample test and the NPs suspension can be due to a less availability of the medium molecules for chemical reactions; they formed the double electrical layer to prevent NPs agglomeration. Tomato seeds are more sensitive to the environment and the negative effects were more pronounced than the results obtained for lettuce and cucumber seeds, although they present the same trend. Racuciu et al. [40] found that low concentrations of aqueous ferrofluid (NPs coated with TMAOH) stimulated plant growth while high concentrations induced inhibitory or toxic effects on the growth of young popcorn plants, but the effect of the TMAOH on these results was not studied. Barrena et al. [24] concluded that the toxic effects observed in NPs can be due to the presence of NPs-solvent (stabilizers) and to the combined effect of NPs-solvent and NPs. The effect observed in the germination index is attributed exclusively to the decrease in root length; for this reason is recommended to present the root length and germination test results separated when using this type of tests.

3.5.2. TiO_2 NPs

Significant reduction on lettuce germination index (GI) were detected in the samples of TMAOH medium with 2.5 mg/l Pb^{2+} in solution (74±9 %) as well as in root elongation (77±5 %); slight promotion of root elongation was observed in the case of seeds immersed in NPs with lead adsorbed (107±3 %). In the case of tomato the effect was more accentuated with 62±4 % of GI for TMAOH medium, and 47±4 % for solvent and lead solution. The NPs suspension, the NPs suspension after Pb^{2+} adsorption and the liquor obtained after NPs separation process presented no effect on germination and root elongation test.

3.5.3. CeO_2 NPs

In the three seeds studied (Table 5), a decrease in germination index (GI) was observed mainly via root elongation diminution in tomato (51±10 %), cucumber (63±14%) and lettuce (75±7 %). For the HMT medium, high phytotoxicity was observed for CeO_2 NPs suspension in tomato (4±1 %), cucumber (1±0 %) and lettuce (4±1 %). CeO_2 NPs with Pb^{2+} adsorption suspension showed similar results for tomato (2±0 %), cucumber (2±1 %) and lettuce (4±1 %). Liquor obtained after NPs centrifugation presented: tomato 2±0 %, cucumber 2±0 % and lettuce 2±1 %. The CeO_2 NPs are responsible for the high toxicity presented in the three cases; even when the NPs were centrifuged the liquor presented high toxicity. The toxic effect obtained after centrifugation process indicated the presence of a toxic compound liberated or formed in solution during the process. López-Moreno et al. [41] studied the toxic effects of nanoceria as a function of concentration, in four edible plant species. Variable phytotoxicity results were obtained: stimulated growth root in cucumber, a decreased effect in corn and tomato, relatively low toxicity on seed germination of alfalfa and cucumber and moderate toxicity on tomato and corn. These differences in the toxic effects could be attributed to the NPs synthesis method, the morphology, the surface reactivity and the molecule used as stabilizer medium, which has been observed to play an important role.

At the lead concentration analyzed (2.5 Pb^{2+} mg/l) no phytotoxic effect was observed, although high toxicity against *Photobacterium phosphoreum* was previously obtained. In general the seeds of tomato were more sensible at these experimental conditions than cucumber and lettuce seeds.

3.5.4. Summary of germination results

The results presented in Table 5 on the germination test emphasize that different seeds present different responses to different nanoparticles exposure. Moreover, the level of dispersion found makes these results difficult to interpret. The role of the nanoparticles stabilizer should be carefully considered. In conclusion, this kind of test does not seem suitable to have a quick evaluation of nanoparticles toxicity.

4. Conclusions

The adsorption capacity of Pb^{2+} using CeO_2, TiO_2 and Fe_3O_4 NPs was determined. The best value for these NPs of similar particle size was for CeO_2. The toxic evaluation of each element evolved in the NPs stabilization and process is necessary to understand the possible impact and prevent ecological damage. The solvents/stabilizers used for the NPs stabilization showed phytotoxicity. In further NPs synthesis, the stabilization medium has to be changed to reduce this impact. Cerium NPs presented a high level of lead removal although showed a high phytotoxicity. The toxicity presented by the liquor after separation indicated a dissolution process with toxic effects to marine bacteria used in the Microtox test and in the germination test in tomato, lettuce and cucumber seeds. Further studies must be carried out to understand the phytotoxic mechanism of CeO_2 NPs. The effect of the stabilizer used in NPs synthesis has also to be studied to understand these complex mechanisms. TiO_2 and Fe_3O_4 NPs did not present toxicity and can be used as absorbents for Pb (II) removal due to the high adsorption obtained and the short adsorption time needed to achieve equilibrium.

Acknowledgements

Financial support was provided by the Spanish Ministerio de Medio Ambiente y Medio Rural y Marino (Project Exp. 007/RN08/03.1). Sonia Recillas thanks Universitat Autònoma de Barcelona for the award of a post-doctoral fellowship.

References

[1] B. Nowack, T.D. Bucheli, Occurrence, behavior and effects of nanoparticles in the environment, Environ. Pollut. 150 (2007) 5-22.

[2] K. Jia, B. Pan, L. Lva, Q. Zhang, X. Wang, B. Pan, W. Zhang, Impregnating titanium phosphate nanoparticles onto a porous cation exchanger for enhanced lead removal from waters, J. Colloid Interface Sci. 331 (2009) 453-457.

[3] W. Förstner, Metal Pollution in the Aquatic Environment, Springer, Berlin Heindelberg, New York, Tokyo (1984) pp. 18-20 (Chapter B: toxic metals).

[4] T. Pradeep, K.R.A. Anshup, Noble metal nanoparticles for water purification: A critical review, Thin Solid Films 517 (2009) 6441-6478.

[5] X. Zhang, S. Lin, X.-Q. Lu, Z. Chen, Removal of Pb(II) from water using synthesized kaolin supported nanoscale zero-valent iron, Chem. Eng. J. 163 (2010) 243-248.

[6] A. Uheida, M. Iglesias, C. Fontàs, M. Hidalgo, V. Salvadó, Y. Zhang, M. Muhammed, Sorption of palladium(II), rhodium(III), and platinum(IV) on Fe_3O_4 nanoparticles, J. Colloid Interface Sci. 301 (2006) 402-408.

[7] N. Strigul, L. Vaccari, C. Galdun, M. Wazne, X. Liu, C. Christodoulatos, K. Jasinkiewicz, Acute toxicity of boron, titanium dioxide, and aluminum nanoparticles to *Daphnia magna* and *Vibrio fischeri*, Desalination 248 (2009) 771-782.

[8] R. Owen, R. Handy, Formulating the problems for environmental risk assessment of nanomaterials, Environ. Sci. Technol. 41 (2007) 5582-5588.

[9] R. Behra, H. Krug, Nanoecotoxicology: Nanoparticles at large, Nat. Nanotechnol. 3 (2008) 253–254.

[10] R. Zhang, Y. Niu, Y. Li, C. Zhao, B. Song, Y. Li, Y. Zhou, Acute toxicity study

of the interaction between titanium dioxide nanoparticles and lead acetate in mice, Environ. Toxicol. Pharmacol. 30 (2010) 52-60.

[11] K. Hund-Rinke, M. Simon, Ecotoxic effect of photocatalytic active nanoparticles (TiO_2) on algae and daphnids, Environ. Sci. Pollut. Res. 13 (2006) 225-232.

[12] Nanotechnology white paper. Document Number EPA 100/B-07001 1 February 2007, United States Environmental Protection Agency.

[13] M. Ruffini, Castiglione, R. Cremonini, Nanoparticles and higher plants, Caryologia 62 (2009) 161-165.

[14] J. Turkevich, P.C. Stevenson, J. Hillier, Nucleation and growth process in the synthesis of colloidal gold, J. Discuss. Faraday Soc. 11 (1951) 55-75.

[15] F. Zhang, Q. Jin, S.W Chan, Ceria nanoparticles: Size, size distribution, and shape, J. Appl. Phys. 95 (2004) 4319-4326.

[16] A. Pottier, S. Cassaignon, C. Chaneac, F. Villain, E. Tronca, J.P. Jolivet, Size tailoring of TiO_2 anatase nanoparticles in aqueous medium and synthesis of nanocomposites. Characterization by Raman spectroscopy, J. Mater. Chem. 13, (2003) 877-882.

[17] R. Massart, Preparation of Aqueous Magnetic Liquids in Alkaline and Acidic Media, IEEE Transactions on Magnetics. 17 (1981) 1247-1248.

[18] J.P. Jolivet, R. Massart, J.M. Fruchart, Synthesis and physicochemical study on nonsurfactant magnetic colloids in aqueous medium, Nouveau J. De Chimie-New J. Chem. 7 (1983) 325-331.

[19] A. Greenberg, J. Connors, D. Jenkins, Standard methods for the examination of water and wastewater. 15th ed. American Public Health Association, USA. 1981, pp. 187-190.

[20] N. Nashaat, N. Nassar, Rapid removal and recovery of Pb(II) from wastewater by magnetic nanoadsorbents, J. Hazard. Mater. 184 (2010) 538-546.

[21] A. Uheida, M. Iglesias, C. Fontàs, M. Hidalgo, V. Salvadó, Y. Zhang, M. Muhammed, Sorption of palladium(II), rhodium(III), and platinum(IV) on Fe_3O_4 nanoparticles, J. Colloid Interface Sci. 301 (2006) 402-408.

[22] A. Uheida, G. Salazar-Alvarez, E. Björkman, Z. Yu, M. Muhammed, Fe_3O_4 and g-Fe_2O_3 nanoparticles for the adsorption of Co^{2+} from aqueous solution, J. Colloid Interface Sci. 298 (2006) 501-507.

[23] H. Sun, X. Zhang, Q. Niu, Y. Chen, J. Crittenden, Enhanced accumulation of arsenate in carp in the presence of titanium dioxide nanoparticles, Water Air Soil Pollut. 178 (2007) 245-254.

[24] R. Barrena, E. Casals, J. Colón, X. Font, A. Sánchez, V. Puntes, Evaluation of model nanoparticles eco-toxicity, Chemosphere 75 (2009) 850-857.

[25] DIN 38412, part 34, 1991. Determination of the inhibitory effect of wastewater on the light emission of *Photobacterium phosphoreum* (test using preserved luminescent bacteria).

[26] R.N. Coleman, A.A.Q. Qureshi, Microtox and spirillum volutans tests for assessing toxicity of environmental samples, Bull. Environ. Contam. Toxicol. 35 (1985) 443-451.

[27] DIN 38414, 1987. Bestimmung des faulverhaltens (S8). In: Fachgruppe Wasserchemie in der Gesellschaft Deutscher Chemiker und Normausschuss Wasserwesen (NAW) im DIN Deutsches Institut für Normung e.V. (Eds.), Deutsche Einheitsverfahren zur Wasser-, Abwasser- und Schlammuntersuchung, Physikalische, chemische, biologische und bakteriologische Verfahren, VCH Verlagsgesellschaft mbH, Weinheim, Germany.

[28] A.K. Pandey, V. Misra, A.K. Srimal, Removal of chromium and reduction of toxicity to Microtox system from tannery effluent by the use of calcium alginate beads containing humic acid, Chemosphere 51 (2003) 329-333.

[29] M.S. Tiquia, N.F.Y. Tam, I.J. Hodgkiss, Effects of composting on phytotoxicity of spent pig-manure sawdust litter, Environ. Pollut. 93 (1996) 249-256.

[30] The US Department of Agriculture and The US Composting Council, Test methods for the examination of composting and compost, Edaphos International, Houston, 2001.

[31] Y-S. Ho, Review of second-order models for adsorption systems, J. Hazar. Mater. B136 (2006) 681-689.

[32] Y.S. Ho, G. McKay, The kinetics of sorption of divalent metal ions onto sphagnum moss peat, Water Res. 34 (2000) 735-742.

[33] X. Xie, L. Gao, Effect of crystal structure on adsorption behaviors of nanosized TiO_2 for heavy-metal cations, Appl. Phys. 9 (2009) S185–S188.

[34] X. Zhao, Q. Jia, N. Song, W. Zhou, Y. Li, Adsorption of Pb(II) from an Aqueous Solution by Titanium Dioxide/Carbon Nanotube Nanocomposites: Kinetics, Thermodynamics and Isotherms, J. Chem. Eng. Data, 55 (2010) 4428-4433.

[35] R.J. Griffitt, J. Luo, J. Gao, J.C. Bonzongo, D.S. Barber, Effects of particle composition and species on toxicity of metallic nanomaterials in aquatic organisms, Environ. Toxicol. Chem. 27 (2008) 1972–1978.

[36] M. Heinlaan, A. Ivask, I. Blinova, H.-C. Dubourguier, A. Kahru, Toxicity of nanosized and bulk ZnO, CuO and TiO_2 to bacteria *Vibrio fischeri* and crustaceans *Daphnia magna* and *Thamnocephalus platyurus*, Chemosphere, 71 (2008) 1308-1316.

[37] P. Pärt, G. Wilmark, The influence of some complexing agents (EDTA and Citrate) on the uptake of cadmium in the perfused rainbow trout gills, Aquat. Toxicol. 5 (1984) 277-289.

[38] D.E. Giammar, C.J. Maus, L. Xie, Effects of Particle Size and Crystalline Phase on Lead Adsorption to Titanium Dioxide Nanoparticles, Environ. Eng. Sci. 24, (2007) 85-95.

[39] A.T. Stone, A. Torrents, J. Smolen, D. Vasudevan, J. Hadley, Adsorption of organic-compounds possessing ligand donor groups at the oxide water interface, Environ. Sci. Technol. 27, (1993) 895-909.

[40] M. Racuciu, D. Creanga, TMA-OH coated magnetic nanoparticles internalized in vegetal tissue, Rom. J. Phys. 52 (2007) 395-402.

[41] M.L. Lopez-Moreno, G. De La Rosa, J.A. Hernandez-Viezcas, J.R. Peralta-Videa, J.L. Gardea-Torresdey, X-ray Absorption Spectroscopy (XAS) Corroboration of the Uptake and Storage of CeO_2 Nanoparticles and Assessment of Their Differential Toxicity in Four Edible Plant Species, J. Agric. Food Chem. 58 (2010) 3689-3693.

Tables

Table 1. Main characteristics of the used nanoparticles as they were synthesized.

Nanoparticle composition	Shape	Z-Potential (mV)	Surface coating	Concentration (NPs/mL)	Concentration (mg/mL)	Solvent Conc. (mM)
Iron Oxide (Fe_3O_4)	Irregular	-58	Inorganic TMAOH*	~10^{15}	0.67	TMAOH 1
Cerium Oxide (CeO_2)	Irregular	+12	Inorganic HMT*	~10^{16}	0.64	HMT 8.33
Titanium Oxide (TiO_2)	Irregular	-42	Inorganic TMAOH*	~10^{16}	1.2	TMAOH 10

* TMAOH: Tetramethylammonium hydroxide
* HMT: Hexamethylenetetramine

Table 2. Adsorption capacity (mg Pb^{2+}/g NPs) after 24 hours of reaction, Pb^{2+} removal (%) and equilibrium Pb^{2+} concentration (mg/l) of CeO_2, TiO_2 and Fe_3O_4 NPs.

NPs	Pb^{2+} Initial conc. (mg/l)	NPs concentration (mg/l)	Pb^{2+} equilibrium conc. (mg/l)	q(t) 24 h (mg Pb/g NPs)	Pb^{2+} removal (%)
CeO_2	3.4	320	N.D*	10.3	~100
CeO_2	8.5	320	N.D*	26.6	~100
CeO_2	17	320	3.9	41.0	77.3
CeO_2	95	320	37.0	181.2	58
TiO_2	3.4	560	N.D*	6.1	~100
TiO_2	8.5	560	4.2	7.8	51.1
TiO_2	17	560	10.8	11.0	36.2
TiO_2	95	320	64.8	153.2	49.2
Fe_3O_4	3.4	335	N.D*	10.1	~100
Fe_3O_4	8.5	335	N.D*	25.4	~100
Fe_3O_4	17	335	N.D*	50.7	~100
Fe_3O_4	95	320	68.9	81.6	26.1

* N.D: not detected

Table 3. Maximum adsorption capacity at equilibrium and pseudo-second-order rate constants (k_2) obtained using the pseudo-second-order kinetic model. Concentration of NPs of CeO_2, Fe_3O_4 and TiO_2 was 320 mg/l and initial Pb^{2+} concentration was 100 mg/l.

NPs	Concentration (mg/l)	q_e ($mgPb^{2+}$ /g NPs)	k_2 (g CeO_2/(mg Pb^{2+} h))	R^2
CeO_2	320	188.70	0.035	0.991
Fe_3O_4	320	82.64	0.012	0.986
TiO_2	320	158.73	0.004	0.982

Table 4. The IC50 obtained by Microtox assay at 15 minutes for Fe_3O_4, CeO_2 and TiO_2 NPs, NPs oxides with lead adsorbed (2.5 mg/l Pb^{2+}) and the liquor obtained when NPs with lead adsorbed was centrifuged.

Compound	IC50
NPs Fe	44.8
NPs Fe+Pb	50.5
Liquor NPs Fe	163.2
NPs Ce	35.2
NPs Ce+Pb	38.7
Liquor NPs Ce	35.7
NPs Ti	no toxic
NPs Ti+Pb	no toxic
Liquor NPs Ti	no toxic
Initial Pb solution (2.5mg/l Pb^{2+})	0.1

Table 5. Influence of nanoparticle samples on germination index (GI) and root growth for Lettuce (*Lactuca sativa*), Tomato (*Lycopersicom esculentum)* and Cucumber *(Cucumis sativus)* seeds. Significant difference was marked with asterisk (*) ($p \leq 0.05$).

	Fe_3O_4 NPs		TiO_2 NPs		CeO_2 NPs	
Species	GI (%)	Root elongation (%)	GI (%)	Root elongation (%)	GI (%)	Root elongation (%)
Lettuce						
Distilled water	97±3	100±0	97±3	100±0	97±3	100±0
Solvent	61±1*	67±2*	88±12	91±7	75±7*	82±5*
Solvent + Lead	64±3*	74±11*	74±9*	77±5*	74±5*	76±3*
NPs	84±5	89±4*	97±10	104±4	4±1*	4±7*
NPs-Pb	94±9	108±3	105±1	107±3*	4±1*	5±1*
NPs-Pb liquor	106±10	112±13	98±17	105±19	2±1*	3±1*
Tomato						
Distilled water	87±3	100±0	87±3	100±0	87±3	100±0
Solvent	42±12*	46±10*	62±4*	64±3*	51±10*	526±7*
Solvent + Lead	41±5*	43±3*	47±3*	52±1*	74±24	88±17
NPs	61±3*	66±4*	85±16	97±10	5±1*	5±2*
NPs -Pb	67±15	69±12*	78±11	90±11	2±0*	4±0*
NPs-Pb liquor	81±8	87±6	84±7	101±18	2±0*	4±0*
Cucumber						
Distilled water	97±6	100±0	976	100±0	97±6	100±0
Solvent	76±16	88±19	103±14	111±21	63±14	70±9
Solvent + Lead	81±14	86±10	86±12	88±8	72±12	72±12
NPs	78±10	82±16	103±16	107±18	1±0*	2±0*
Fe_3O_4-Pb NPs	96±22	99±19	91±9	94±9	2±1*	2±1*
Fe_3O_4-Pb NPs liquor	95±12	98±8	109±21	116±20	2±0*	2±1*

Legends to Figures

Figure 1.- Characterization of the NPs used in this work. Left: TEM image and size distribution (inset) and right: XRD spectrum, as characteristic signatures of these NPs.

Figure 2.- Pb^{2+} adsorption evolution at pH=7 and room temperature. Fe_3O_4 (square), CeO_2 (circle) and TiO_2 (triangle). Initial Pb concentration was 95 mg/l and initial concentration of NPs was 320 mg/l.

Figure 3.- Pseudo-second-order model: Pb^{2+} adsorption by Fe_3O_4 (squares), CeO_2 (circles) and TiO_2 (triangles).

Fig. 1

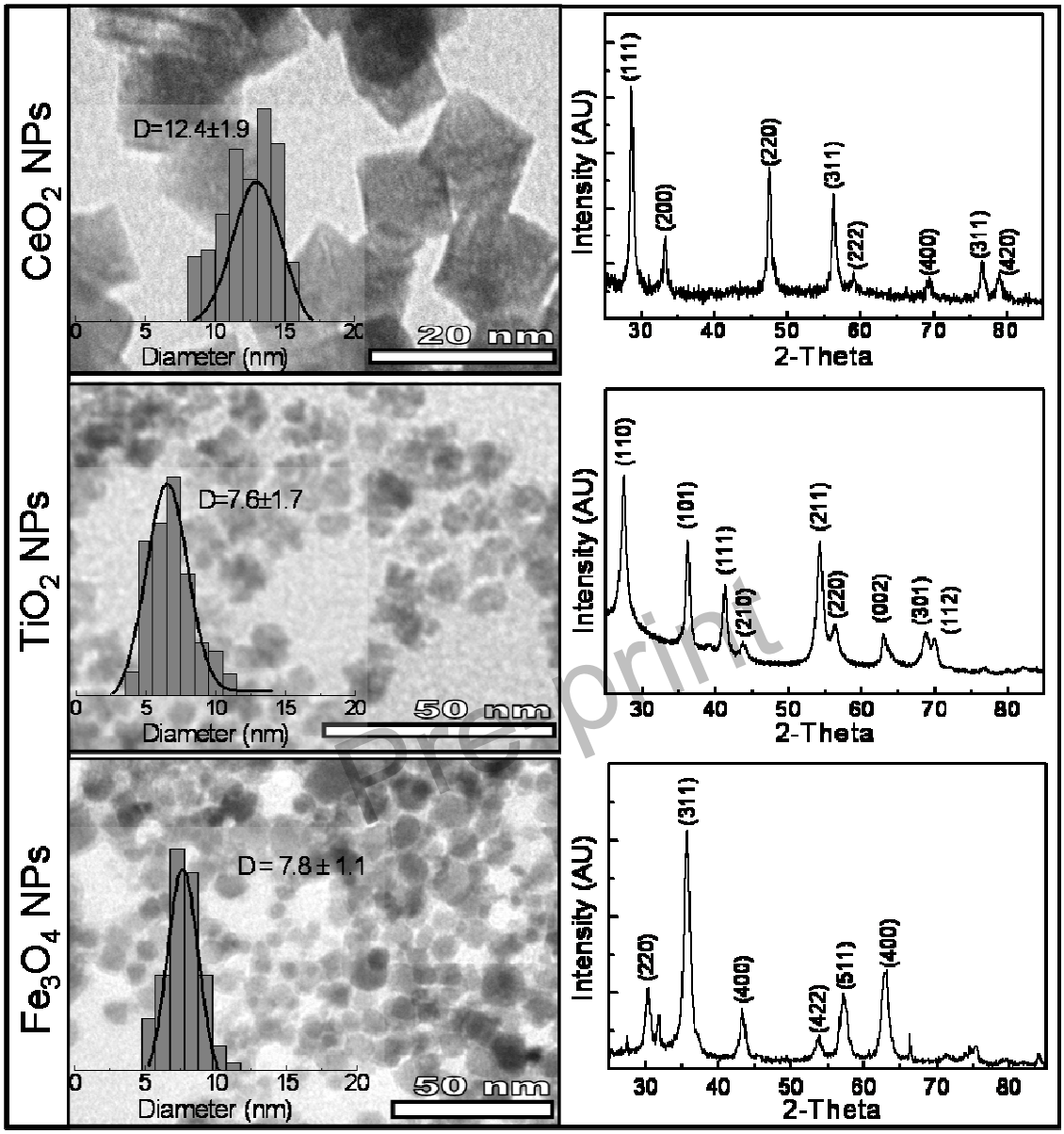

Fig. 2

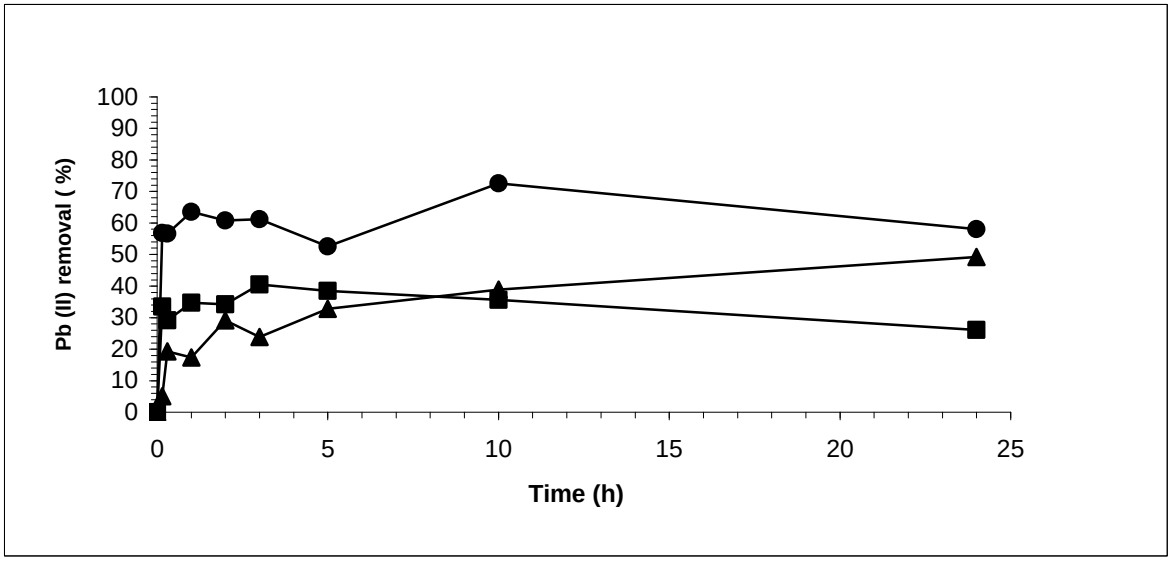

Fig. 3